Published in final edited form as:

Cancer Res. 2011 August 1; 71(15): 5075–5080. doi:10.1158/0008-5472.CAN-11-0247.

Mechanical stiffness grades metastatic potential in patient tumor cells and in cancer cell lines

Vinay Swaminathan[1,*], **Karthikeyan Mythreye**[2,*], **E Tim O'Brien**[3], **Andrew Berchuck**[4], **Gerard C Blobe**[2,#], and **Richard Superfine**[3,#]

[1]Curriculum in Applied Science and Engineering, UNC Chapel Hill, NC

[2]Department of Medicine, Duke University Medical Center, Durham, NC

[3]Department of Physics and Astronomy, UNC Chapel Hill, NC

[4]Department of Gynecology and Obstetrics, Duke University Medical Center, Durham, NC

Abstract

Cancer cells are defined by their ability to invade through the basement membrane, a critical step during metastasis. While increased secretion of proteases, which facilitates degradation of the basement membrane, and alterations in the cytoskeletal architecture of cancer cells have been previously studied, the contribution of the mechanical properties of cells in invasion is unclear. Here we apply a magnetic tweezer system to establish that stiffness of patient tumor cells and cancer cell lines inversely correlates with migration and invasion through three-dimensional basement membranes, a correlation known as a power law. We found that cancer cells with the highest migratory and invasive potential are five times less stiff than cells with the lowest migration and invasion potential. Moreover, decreasing cell stiffness by pharmacological inhibition of myosin II increases invasiveness, while increasing cell stiffness by restoring expression of the metastasis suppressor TβRIII/betaglycan decreases invasiveness. These findings are the first demonstration of the power law relation between the stiffness and the invasiveness of cancer cells and show that mechanical phenotypes can be used to grade the metastatic potential of cell populations with the potential for single cell grading. The measurement of a mechanical phenotype, taking minutes rather than hours needed for invasion assays, is promising as a quantitative diagnostic method and as a discovery tool for therapeutics. By demonstrating that altering stiffness predictably alters invasiveness, our results indicate that pathways regulating these mechanical phenotypes are novel targets for molecular therapy of cancer.

Introduction

The spread of cancer from its primary site to distant organs, the "invasion-metastasis cascade", is the main cause of cancer death and invasion of cells into the lymphatics and blood vessels is a crucial step in metastasis, correlating with a poorer patient prognosis [1]. Hallmarks of invasion include secretion of proteases, alterations in adhesion receptors, and changes in cell morphological and migratory properties [2]. Drugs targeting the metastatic cascade, including the matrix metalloproteinases (MMPs), which degrade the extracellular matrix, or the migratory machinery, are being evaluated in clinical trials [3] but results have been disappointing potentially due to the complexity and redundancy of the metastatic cascade.

Corresponding Author Richard Superfine, Department of Physics and Astronomy, 345 Chapman Hall, UNC, Chapel Hill, NC 27599-3255, Ph: 919.962.1185, Fax: 919.962.0480, rsuper@physics.unc.edu.

*#These authors contributed equally to this work.

Cell stiffness has been postulated to play roles in transmigration of cancer cells through a basement membrane [4]. A variety of biophysical techniques including membrane stretching, atomic force microscopy, optical traps and micropipette aspiration have been used to probe the mechanical properties of cells [5]. These techniques use ferromagnetic or super paramagnetic beads to attach to membrane receptors and are followed by application of either a twisting or a pulling motion to the bead and thus to the cell via an electromagnet [6]. Magnetic tweezers, like the one described here, provides for a wide range of force magnitudes (10pN-10nN), the ability to probe individual cells and to perform measurements in minutes to understand the time dependent development of a cell's mechanical state [7]. While cancer *tissue* has been found to be generally stiffer than normal tissue, recent studies have shown that cancer *cells* themselves are more compliant than normal cells [8]. However, the extent of the correlation between mechanical properties and specific aspects of cancer progression has not been determined. Specifically, whether modification of cell stiffness might alter key aspects of metastasis such as invasion is unclear. The measurement of metastatic potential through two dimensional substrates (migration; movement through membrane pores) and three dimensional motion through tissue matrix material (invasion) are common assays used in cancer cell biology and applied as population studies over longer time durations. Therefore, it is of broad interest from an analytical, diagnostic and cancer biology context to understand how a mechanical phenotype measure could be utilized relative to current metastatic potential assays. To address these questions, we have used a magnetic tweezer system in parallel with Matrigel invasion assays to examine the specific correlation between mechanical properties of cancer cells and their metastatic potential, specifically their invasive potential.

Materials and Methods

Cell culture and Reagents

Human ovarian cancer cell lines, OVCA429, IGROV, SKOV3, HEY, DOV13, OV2008, Ovca420 and ovarian cancer stable cells lines, Ovca429Neo, Ovca429 TβRIII were cultured, derived, and characterized as previously described [9]. Antibody to pMLC (myosin light chain) was obtained from Cell Signaling Technologies (Cat. No. 3671) and pan-cytokeratin antibody was obtained from Santa Cruz (Cat. No. 81714).

Isolation of cancer cells from Ascites

Primary short term epithelial ovarian cancer cell cultures were established from the ascites of patients with Stage III/IV epithelial ovarian cancer as described previously [10]. Cells were seeded and grown on 10 μg/mL fibronectin coated culture dishes in RPMI media containing 20% FBS and 1% penicillin/streptomycin solution at 37C in 5% CO2. Adhered cells were subject to limited dispase digestion for the first passage to remove fibroblasts and stained with a pan-cytokeratin antibody to confirm epithelial origin.

Immunoflourescence

Immunoflourescence was performed essentially as described previously [9] and images were obtained using a Nikon inverted microscope.

Matrigel invasion and Transwell Migration assays

Cancer cells were seeded at a cell density of 25,000–70,000 on either Matrigel coated or uncoated filters and allowed to invade for 18 – 24 hours towards 10% FBS in the lower chamber. Cells invading and migrating through the Matrigel layer were visualized and counted as described [9]. Percent cell migration or invasion was determined as the fraction of total cells that invaded through the filter. Blebbistatin (100μm) [10] where used, was added to

the top chamber of the transwell and migration and invasion allowed to proceed. Each assay was set up in duplicate, and each experiment was conducted at least 3 times with 4 random fields from a 10× magnification analyzed for each membrane.

Magnetic Tweezers Assay

The three Dimensional Force Microscope (3DFM) [11] was used for applying controlled and precise 60–100 pN local force (Figure S1) on 2.8 micron magnetic beads (DYNAL Biotech, Oslo, Norway) coated with fibronectin (Sigma Aldrich, St. Louis, MO). Briefly, cells were plated on coverslips followed by addition of the beads. Cells and beads were incubated for 30 minutes followed by force application and resultant bead displacements were recorded and analyzed. The displacement of the beads was recorded with high-speed video camera (Pulnix, JAI, Ca) and tracked using Video Spot Tracker (hhtp://cismm.cs.unc.edu). The mean creep compliance was calculated from the tracked displacements as described. Spring constants were derived by fitting the compliance curves to a Jeffrey's model for viscoelastic liquids (Figure S1). For pharmacological experiments, blebbistatin, (100μm) was added to the cells for 30 mins, prior to addition of the beads and the reagent left in for the remainder of the experiment.

Results and Discussion

The invasiveness and migratory capacity of a panel of ovarian cancer cell lines and primary cells derived from ascites of patients with advanced stage ovarian cancer was determined using transwell assays in the presence or absence of reconstituted Matrigel (Methods, Figure S2). While both ovarian cancer cell lines and primary cancer cells were able to invade through Matrigel, the degree of invasiveness varied widely among individual lines, with the most invasive and migratory cell line, HEY, being two orders of magnitude more invasive (I_{HEY}= 0.85%, I_{IGROV}= 0.006%) than the least migratory and invasive cell line, IGROV (Figure 1A). Similarly, while primary cells were obtained from patients at either stage III or stage IV disease (Supp. Table 1), the most invasive primary cell line, OV207, was an order of magnitude more invasive than the least invasive primary cell line, OV445 (Figure 1B; I_{OV207} = 0.193%, I_{OV445}= 0.006%). Mechanical properties of the cancer cells from the same passage as used for invasion studies were determined in parallel using a three dimensional force microscope (3DFM) based magnetic tweezer system [11]. The creep compliance (deformability) was calculated as the average time dependent deformation normalized by the constant stress applied ($J_{\max}=\frac{r_{\max}\times 6\pi a}{F}$, where a is the radius of the bead and r_{max} is maximum bead displacement). We find that the most invasive cell line, HEY, was 10 times more deformable than the least invasive cell line IGROV. In addition, OV207 that exhibited 30 fold greater invasion than OV445, had a J_{max}= 3.1 Pa^{-1} in contrast with the J_{max}= 0.3 Pa^{-1} observed for OV445 (Figure 1C & 1D). Hence both cell lines and primary cells that exhibited high invasive behavior also presented high J_{max} values and were more compliant. To further examine the relationship between cancer cell deformability and invasive potential, the effective shear modulus (here on referred to as the stiffness, k), of the cell was calculated by fitting a modified Kelvin Voigt model [12] to the compliance using a least squares fit (see Supp Mat.). The cancer cell lines and primary cells were classified both by their stiffness and their invasiveness, with both parameters falling into three classes of low, medium and high stiffness or invasiveness, respectively. Cell lines within a given class did not exhibit statistically significant differences in their stiffness, while cell lines between classes, were significantly different ($p \leq 0.05$). Consistent with previous findings, the distribution of all stiffness values for the less invasive cell line (IGROV) showed a log normal distribution whereas the highly invasive cell line (Skov3) showed a normal distribution (Figure S4) [8]. Scaling the cell line and primary cell correlations separately with

their respective highest cell stiffness values resulted in a single parameter power law (Figure 2D). A similar correlation and power law was also observed for stiffness and cell migration (Figure S2)($p_{\text{cell lines}} = -0.95$ and $p_{\text{primaries}} = -0.96$ in log log scale). While previous reports have demonstrated alterations in cell stiffness of cancer cells either from body fluids or tumors [13], our data using ovarian cancer cell lines and cells from patient ascites demonstrate that cancer cells across a given disease population exhibit a varying degree of stiffness, a phenomenon previously not described. In addition, the variability in stiffness correlates directly with a specific measure of metastatic progression as determined using in vitro three-dimensional invasion assays.

Stiffness and deformation are strongly regulated by actomyosin contractility [14,15]. Phosphorylation of the 20kD regulatory myosin light chain (MLC) subunit on the Ser19 (mono) or on Ser19/Thr18(di) [16] has been shown to promote cell contractility via changes in the actin myosin network[17]. Visualization of actin in the stiffest and least invasive cell line, IGROV, revealed strong cortical actin staining with little to no cell protrusions or lamellipodial structures (Figure 3A). In contrast, the compliant and invasive cell lines, including SKOV and HEY cells, exhibited distinct lamellipodial and protrusive structures with limited cortical actin. In addition, phosphorylated myosin light chain (pMLC) was found distinctly along the cell periphery in IGROV's (Figure 3B) while SKOV3 and HEY cells had little to no peripheral pMLC localization. This phenotypic difference between the stiffest/least invasive and the compliant/most invasive cell lines might reflect differences in epithelial character of the cells. Accordingly, we examined the expression of an epithelial marker (E-Cadherin) and a mesenchymal marker (Vimentin) in these cell lines. Indeed, the stiffest/least invasive cell lines expressed more E-Cadherin and less Vimentin, while the compliant/most invasive cell lines expressed less E-Cadherin and more Vimentin (Figure S5). Intriguingly, while the Ovca420 and IGROV cells both exhibited high cortical actin (Figure 3A and 3B), high E-Cadherin expression and low Vimentin expression (Figure S5), they exhibited a 1.7 fold difference in stiffness, which corresponded to a 4-fold difference in invasion (Figure 1 and 2). These data demonstrate that cell stiffness measurements performed as described may be a more discerning measurement of metastatic potential than examining cell structure or epithelial character. To investigate the role of stiffness as impacted by the cytoskeleton on migration and invasion, we determined the effect of altering acto-myosin contractility on these properties. Since cells with differential invasiveness (IGROV vs. HEY) had distinct pMLC localization and cytoskeletal architecture (Figure 3), we used blebbistatin, a Myosin II inhibitor on the stiffest cell line (IGROV) and examined the effect on cell stiffness, migration and invasion. Blebbistatin, at a concentration that disrupted cortical pMLC localization but did not affect viability, increased cell invasion by 2.5 fold, cell migration by 4 fold and decreased cell stiffness by 2 fold (Figure 4C and 4D). We also observed concomitant alterations in the actin cytoskeleton of IGROV cells (Figure S3), supporting a relationship between actomyosin contractility, cell stiffness and invasion of cancer cells. Another factor implicated in regulating migration and invasion either via the cytoskeleton or via secretion of proteases like MMPs is transforming growth factor-β (TGF-β) [18]. Early in carcinogenesis tumours become resistant to the homeostatic effects of TGF-β. One of the proposed mechanisms is loss of expression of the type III TGF β receptor (TβRIII), which has been demonstrated in a number of human cancers, including cancers of the breast, lung ovary, pancreas and prostate (reviewed in [18] TβRIII has been demonstrated to regulate cancer cell motility via alterations in the actin cytoskeleton [9]. To further investigate the contribution of the cytoskeleton and stiffness on cancer cell invasion, we examined the effect of TβRIII expression on cancer cell stiffness using stable cell lines Ovca429Neo, (no TβRIII expression), and Ovca429TβRIII, (TβRIII expression restored) [9]. We found that Ovca429TβRIII cells were two-fold stiffer than Ovca429Neo cells ($K_{\text{ovca429-T}\beta\text{RIII}} = 2.9$Pa, $K_{\text{Ovca429-Neo}} = 1.29$ Pa; Figure 4B). Further, this increase in stiffness corresponded to a decrease in invasiveness, similar to the correlation

observed in the cancer cell lines (Figure 4A). In addition, treating Ovca429TβRIII cells with blebbistatin increased their invasiveness by four fold and decreased the stiffness by two fold ($K_{ovca429\text{-}T\beta RIII\text{-}blebbistatin} = 1.48Pa$, $I_{ovca429\text{-}T\beta RIII\text{-}blebbistatin} = 0.04\%$) similar to effects seen with blebbistatin treatment of the stiffest ovarian cancer cell line, IGROV (Figure 4C and 4D). Hence, cytoskeletal stiffness and effects on myosin II function may mediate suppression of migration and invasion by TβRIII.

Our results are the first evidence that metastatic potential measured through cancer cell invasion shows an inverse power-law relationship with cell stiffness. The particular exponent we derive may depend on the methodology employed for mechanical property determination. As cancer cells get progressively more invasive, they display softer mechanical characteristics that result in cell deformation and shape changes suitable for a metastatic population. We also find that cell lines having similar cytomorphology and cells from patients with similar stage disease can have widely different invasive potential that correlates with differences in stiffness. Currently, cell based diagnoses in cancer rely on histology examination of the removed tissue sample through antibody labeling of specific markers. This complex process is not always reliable and lacks quantified assessment of the disease state. Hence, sensitive biophysical measurements such as those demonstrated here, can be performed in short periods of time, on samples obtained from either ascites or circulating cells, providing potentially unique information about the patient's cancer including metastatic potential. Application of more sophisticated models to quantify scale free cell mechanics will provide further insight into this relationship [19,20]. These insights into biomechanical changes during cancer progression have the potential to lead to novel therapy for treatments. Our observation that the relationship between invasiveness and stiffness is maintained across a series of cancer cell lines, in patient tumor specimens, and under cell biochemical modifications that increase and decrease cell stiffness, suggests that magnetic bead assays for stiffness may be an clinically applicable predictor of invasive potential, and that treatments that affect cellular stiffness, independent of mechanism, may be useful anti-metastatic approaches.

Supplementary Material

Refer to Web version on PubMed Central for supplementary material.

Acknowledgments

We would like to thank Susan Murphy for sharing cancer cell lines and for useful discussions. This work was funded in part by NIH Grant R01-CA135006 (GCB), Department of Defense cancer research grant W81 XWH-09-1-0265 (KM) and P41-EB002025-23A1 (RS) supporting Computer Integrated Systems for Microscopy and Manipulation (CISMM) and Carolina Center for Cancer Nanotechnology Excellence NIH-U54-CA119343 (RS)

References

1. Yilmaz M, Christofori G. EMT, the cytoskeleton, and cancer cell invasion. Cancer Metastasis Rev. 2009; 28:15–33. [PubMed: 19169796]
2. Hanahan D, Weinberg RA. The hallmarks of cancer. Cell. 2000; 100:57–70. [PubMed: 10647931]
3. Decaestecker C, Debeir O, Van Ham P, Kiss R. Can anti-migratory drugs be screened in vitro? A review of 2D and 3D assays for the quantitative analysis of cell migration. Med Res Rev. 2007; 27:149–176. [PubMed: 16888756]
4. Suresh S. Biomechanics and biophysics of cancer cells. Acta Biomater. 2007; 3:413–438. [PubMed: 17540628]
5. Huang H, Kamm RD, Lee RT. Cell mechanics and mechanotransduction: pathways, probes, and physiology. Am J Physiol Cell Physiol. 2004; 287:C1–C11. [PubMed: 15189819]

6. Tim O'Brien E, Cribb J, Marshburn D, Taylor RM 2nd, Superfine R. Chapter 16: Magnetic manipulation for force measurements in cell biology. Methods Cell Biol. 2008; 89:433–450. [PubMed: 19118685]
7. Tanase M, Biais N, Sheetz M. Magnetic tweezers in cell biology. Methods Cell Biol. 2007; 83:473–493. [PubMed: 17613321]
8. Cross SE, Jin YS, Rao J, Gimzewski JK. Nanomechanical analysis of cells from cancer patients. Nat Nanotechnol. 2007; 2:780–783. [PubMed: 18654431]
9. Mythreye K, Blobe GC. The type III TGF-beta receptor regulates epithelial and cancer cell migration through beta-arrestin2-mediated activation of Cdc42. Proc Natl Acad Sci U S A. 2009; 106:8221–8226. [PubMed: 19416857]
10. Katz E, Skorecki K, Tzukerman M. Niche-dependent tumorigenic capacity of malignant ovarian ascites-derived cancer cell subpopulations. Clin Cancer Res. 2009; 15:70–80. [PubMed: 19118034]
11. Fisher JK, et al. Thin-foil magnetic force system for high-numerical-aperture microscopy. Rev Sci Instrum. 2006; 77 nihms8302.
12. Bausch AR, Moller W, Sackmann E. Measurement of local viscoelasticity and forces in living cells by magnetic tweezers. Biophys J. 1999; 76:573–579. [PubMed: 9876170]
13. Remmerbach TW, et al. Oral cancer diagnosis by mechanical phenotyping. Cancer Res. 2009; 69:1728–1732. [PubMed: 19223529]
14. Reichl EM, et al. Interactions between myosin and actin crosslinkers control cytokinesis contractility dynamics and mechanics. Curr Biol. 2008; 18:471–480. [PubMed: 18372178]
15. Stamenovic D, Coughlin MF. The role of prestress and architecture of the cytoskeleton and deformability of cytoskeletal filaments in mechanics of adherent cells: a quantitative analysis. J Theor Biol. 1999; 201:63–74. [PubMed: 10534436]
16. Scholey JM, Taylor KA, Kendrick-Jones J. Regulation of non-muscle myosin assembly by calmodulin-dependent light chain kinase. Nature. 1980; 287:233–235. [PubMed: 6893621]
17. Butcher DT, Alliston T, Weaver VM. A tense situation: forcing tumour progression. Nat Rev Cancer. 2009; 9:108–122. [PubMed: 19165226]
18. Gatza CE, Oh SY, Blobe GC. Roles for the type III TGF-beta receptor in human cancer. Cell Signal.
19. Fabry B, et al. Selected contribution: time course and heterogeneity of contractile responses in cultured human airway smooth muscle cells. J Appl Physiol. 2001; 91:986–994. [PubMed: 11457818]
20. Alcaraz J, et al. Microrheology of human lung epithelial cells measured by atomic force microscopy. Biophys J. 2003; 84:2071–2079. doi:S0006-3495(03)75014-0 [pii]10.1016/S0006-3495(03)75014-0. [PubMed: 12609908]

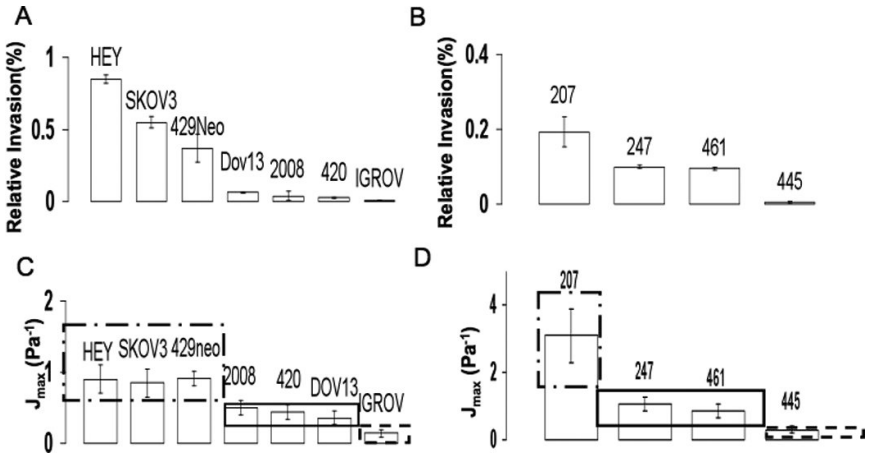

Figure 1. Invasive cancer cells have the highest compliance

A) Invasion assays were performed on the indicated cancer cell lines (Methods) and percent invasion (I) relative to each other presented. Data represent the mean ± SEM of three independent experiments. B) Invasion of primary cancer cells as described in (A). C) Maximum compliance for all the cell lines is presented. The three boxes encompassed by dashed lines indicate the different scored regions based on relative invasion, with cell lines within a box not being statistically significant from each other mechanically ($p \geq 0.05$). (Dash dot box (--)- high invasion, $I \geq 0.4$, Solid box (-)- medium invasion, $0.2 < I < 0.4$, dashed box (---) low invasion, $I \leq 0.2$). D) Maximum compliance for primary cancer cells is presented. The boxes separate statistically significant group of primaries similar to (C). All mechanical measurements represent mean± SEM.

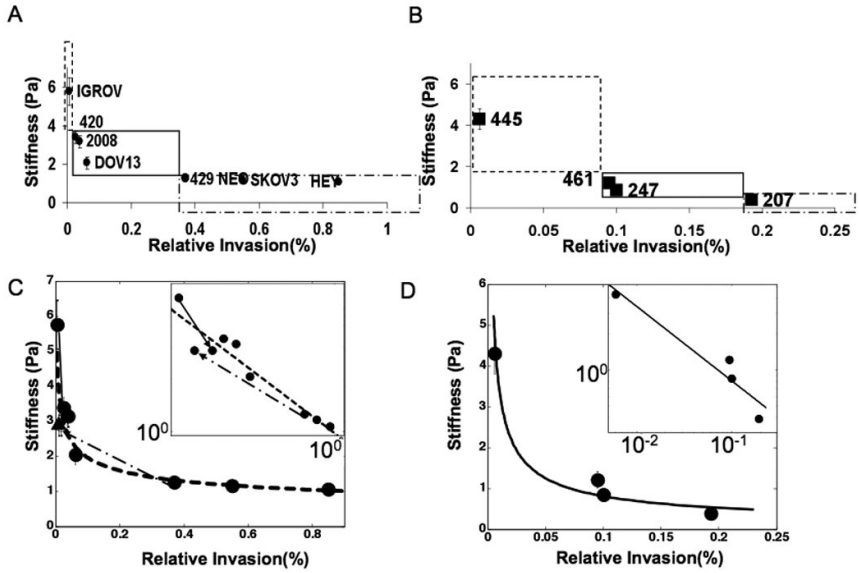

Figure 2. Stiffness correlates with invasion

Stiffness calculated by fitting a modified Kelvin Voigt model (Figure S1) to compliance curves for ovarian cancer cell lines (A) and primary ovarian cancer cells (B) and mapped with the relative invasion from Figure 1A and 1B. The boxes represent the same scored regions as in Figure 1C and 1D. C) Power law showing the correlation between the stiffness of ovarian cancer cell lines and their invasion. IGROV when treated with blebbistatin (open circle, solid arrow) and Ovca429Neo with Ovca429TβRIII (triangle, dash dot arrow) move on the line, consistent with the correlation. (INSET) Power law on log log plot. D) Power law correlation for the primary ovarian cancer cells. (INSET) power law on a log log plot.

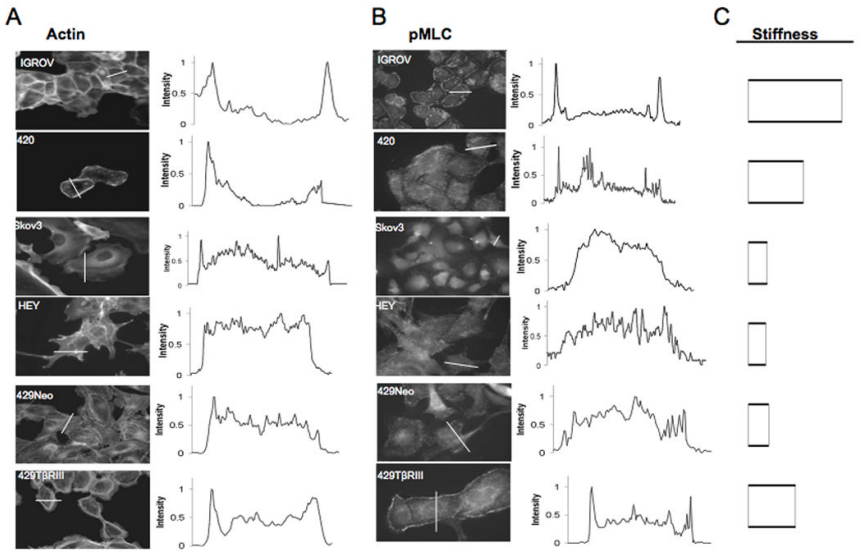

Figure 3. Highly invasive and stiff cancer cells express cortical actin and myosin

Immunoflourescence images of cells stained either for (A) actin using rhodamine conjugated to phalloidin or with an antibody to (B) phosphorylated myosin light chain (pMLC). Quantification of fluorescence intensity using Image J software across the lines shown in the corresponding panels on the left are indicative of stress fiber density in the case of actin or cortical pMLC localization. C) Stiffness of the respective ovarian cancer cell lines.

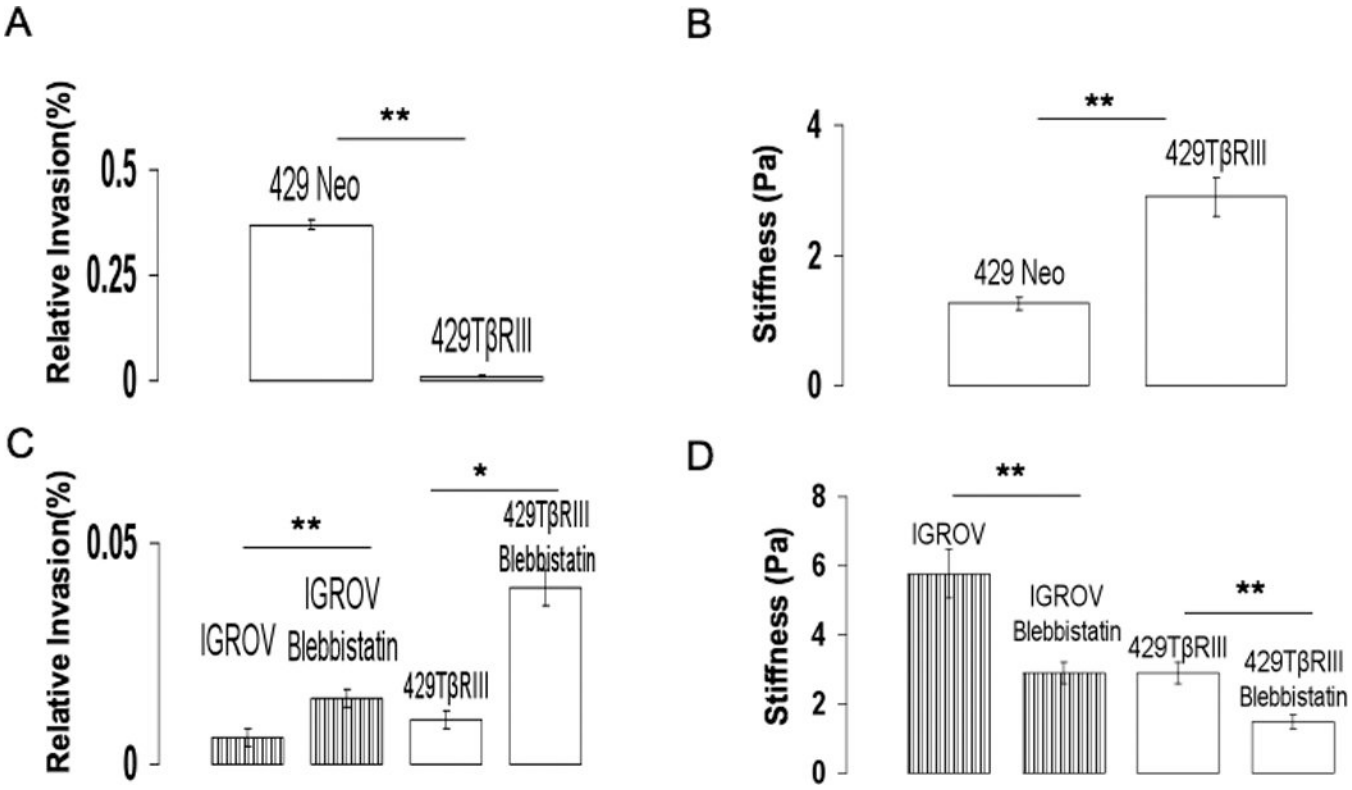

Figure 4. Myosin II function and TβRIII alter stiffness and invasion

A) Invasion assays of Ovca429-Neo and Ovca429-TβRIII was performed as described in Methods and Figure 1. Data are a composite of two independent experiments performed in duplicate. Each column represents the mean ± SEM. B) Stiffness for the corresponding cell type in (A) obtained as described in Methods and Figure 2. C) Effect of blebbistatin treatment on the invasion of IGROV and Ovca429-TβRIII cell types. D) Stiffness for the corresponding cell type and treatments in (C)(** -$p<0.01$,*=$p<0.05$).